Physical Characterization of Solid Iopanoic Acid Forms

WILLIAM C. STAGNER and J. KEITH GUILLORY ˣ

Received December 1, 1978, from the *Division of Pharmaceutics, College of Pharmacy, University of Iowa, Iowa City, IA 52242.* Accepted for publication February 9, 1979.

Abstract □ Three solid forms of iopanoic acid were characterized by X-ray diffraction, differential scanning calorimetry, scanning electron microscopy, thermal microscopy, IR spectroscopy, and dissolution studies. X-ray analysis demonstrated that two solid forms were crystalline and that the third was amorphous. The amorphous form had been reported previously as crystalline. Enthalpies and entropies of transition were calculated using differential scanning calorimetry. A fourth form, a benzene solvate, also was isolated but proved to be too unstable at room temperature to permit conclusive characterization. The amorphous form demonstrated a 10-fold greater intrinsic dissolution rate than the commercially available form (Form I). Form II's intrinsic dissolution rate was 1.5 times greater than that of Form I. In powder dissolution studies, the peak solubilities of the different forms followed the same rank order as their intrinsic dissolution rates. Form II was relatively stable in aqueous saturated solutions, but the amorphous form was rapidly converted to Form I under similar conditions.

Keyphrases □ Iopanoic acid—solid forms, physical characterization, polymorphism, thermal behavior □ Polymorphism—iopanoic acid, physical characterization, thermal behavior □ Radiopaque media—iopanoic acid, solid forms, physical characterization, polymorphism, thermal behavior

Gallbladder disease, a commonly occurring medical problem, is most frequently diagnosed through the use of oral radiographic agents. Over 2,000,000 patients in the United States alone undergo oral cholecystography each year (1). The agent most commonly prescribed to produce gallbladder opacification is iopanoic acid[1] (I), an iodinated organic acid poorly soluble in water; it is administered orally in tablet form.

However, in approximately 25–50% of patients with apparently normal gallbladders, iopanoic acid reaches the gallbladder in insufficient concentration to permit radiographic opacification (1, 2). Consequently, a second examination with another dose of contrast material is often required. Nevertheless, iopanoic acid continues to be widely used because of its ability to permit accurate visualization of gallstones and because of its relatively low toxicity.

BACKGROUND

Inadequate normal gallbladder visualization on initial examination is a complex problem. Ingestion of an insufficient amount of contrast medium, faulty dosing instructions, changes in gastric pH, and decreases in bile flow associated with dietary control are often mentioned as causes for initial nonvisualization. In 1971, Evens *et al.* (3) postulated that poor visualization of normal gallbladders on initial examination was due to incomplete absorption of the radiocontrast medium. They observed large amounts of coarse radiopaque residue on abdominal radiographs of normal patients for whom poor gallbladder opacification had been obtained. Subsequent investigators (4) reported that iopanoic acid exhibited dissolution rate-limited absorption.

Numerous studies (5–8) showed that the sodium salt of iopanoic acid is more rapidly and completely absorbed than the free acid. Sodium iopanoate may react with hydrochloric acid in the stomach to precipitate the free acid as an amorphous material. In a recent investigation, Goldberger *et al.* (9) isolated the precipitated iopanoic acid immediately following acid addition to an aqueous solution of the sodium salt. The dissolution rate of the "freshly precipitated" acid was compared to that of the "dried precipitate," which was assumed to be analogous to the commercially supplied compound. Marked differences in the dissolution rates of the two forms were observed. On examination of the commercial acid, the recent precipitate, and the dried precipitate by oil immersion light microscopy and electron microscopy, the authors concluded that all three forms are crystalline. Consequently, they noted that use of the term "amorphous" to describe the recently precipitated material is not justified.

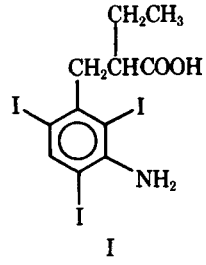

I

The purposes of the present study were: (*a*) to characterize further the previously reported crystalline iopanoic acid forms, and (*b*) to crystallize the material from various solvent systems in an attempt to isolate a polymorph with a rapid dissolution rate that might be stable in the solid state for a reasonable period.

EXPERIMENTAL

Solid Forms—Attempts were made to prepare polymorphs of iopanoic acid by crystallization from various solvent systems using the customary (10) techniques of shock cooling, crystallization at room temperature, and slow crystallization at elevated temperatures. Some 30 samples of crystalline material were examined by thermal microscopy, differential scanning calorimetry, IR spectroscopy, and other techniques, but only in the instances described here were unique crystalline forms obtained.

Commercial iopanoic acid[2] (Form I) was used in the preparation of three other solid forms. A free acid precipitate was obtained by a procedure similar to that described by Goldberger *et al.* (9). Iopanoic acid (3–5 g) was dissolved in 0.1 *N* NaOH, and the final solution pH was adjusted to ~12.5. Nitrogen was bubbled into the solution, and mixing was by a magnetic stirrer. Hydrochloric acid, 0.1 *N*, was added at a rate of 15 ml min^{-1} until the pH reached 2.15. The precipitate was vacuum filtered and stored *in vacuo* (380 mm Hg) for 12 hr at 35°.

In the preparation of Form II, a warm solution of commercial iopanoic acid in analytical reagent grade benzene was frozen rapidly in a dry ice–acetone mixture and then slowly allowed to melt at room temperature. Crystals obtained by filtration of this mixture were identified as a benzene solvate of iopanoic acid. Form II, free of benzene, was obtained when these crystals were stored *in vacuo* (380 mm Hg) for 12 hr at 70°.

X-Ray Analysis—All X-ray data were collected on an automated diffractometer[3] with monochromatized CuKα (λ = 1.5413 Å) radiation. The diffractometer was equipped with a 2θ compensating slit and a graphite monochromator. The instrument was calibrated to within ±0.02° 2θ using the quartz peak at 26.66°. The patterns were recorded both from 2 to 60° 2θ at a scanning speed of 2.4° 2θ min^{-1} and from 6 to 46° 2θ at a scanning speed of 6° 2θ min^{-1}.

Differential Scanning Calorimetry—A thermal analyzer[4], equipped with a differential scanning calorimeter cell, was used to record transition temperatures and heats. Thermograms were recorded simultaneously on an *x–y* recorder[4] and on an external time-base recorder equipped with a mechanical integrator[5]. A 10° min^{-1} heating rate was employed, and a nitrogen purge was maintained throughout each run.

[1] Telepaque, Winthrop Laboratories, New York, N.Y.

[2] Sterling-Winthrop Research Institute, Rensselaer, N.Y.

[3] Phillips APD 3500.

[4] DuPont 900.

[5] Servo/Riter II, Texas Instruments Inc.

0022-3549/79/0800-1005$01.00/0

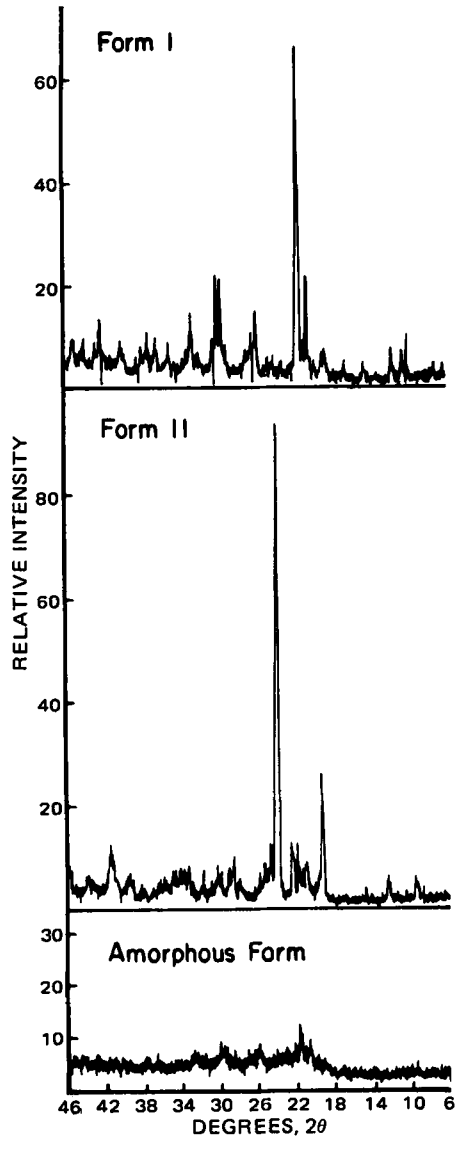

Figure 1—*X-ray powder diffraction patterns of solid iopanoic acid forms.*

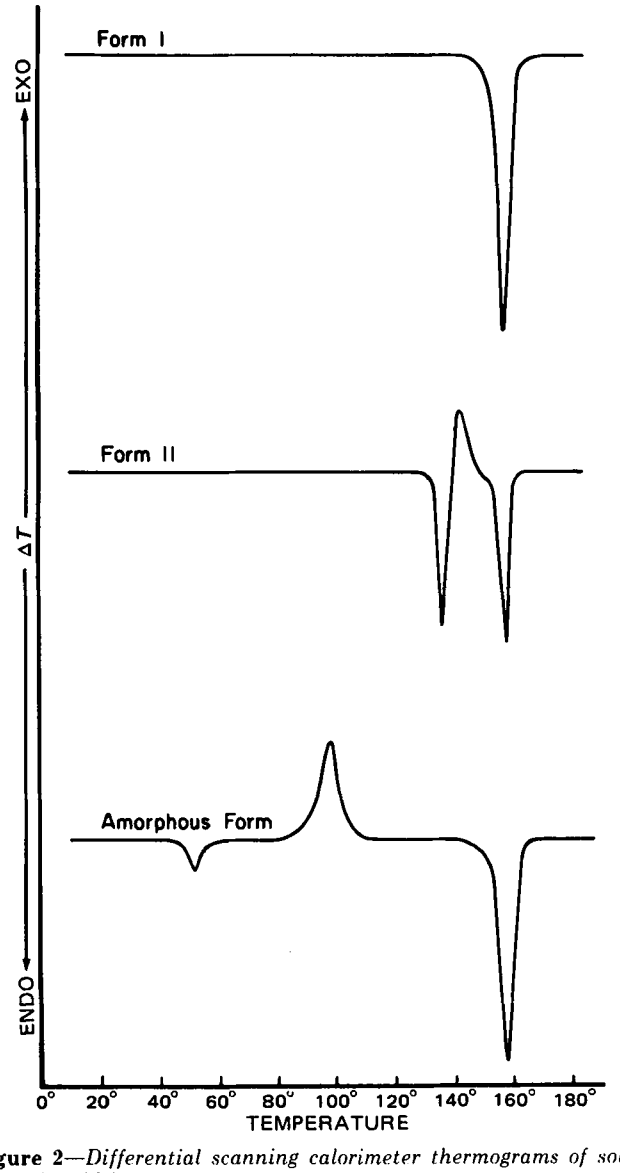

Figure 2—*Differential scanning calorimeter thermograms of solid iopanoic acid forms.*

Area measurements were obtained either by planimetry[6] or from the mechanical integrator trace. When areas were measured by planimetry, a line was drawn from the point at which the thermogram first departed from the baseline to the point, following the transition peak, at which the baseline was resumed.

Benzophenone[7] [ΔH_{fus} 23.5 cal g^{-1}; mp 48.2° (11)], stearic acid[8] (99+%) [ΔH_{fus} 47.5 cal g^{-1}; mp 69.0° (11)], and indium[9] (99.99%) [ΔH_{fus} 6.97 cal g^{-1} (12); mp 156.4° (11)] were used to prepare the calibration curve and to calibrate the temperature axis. The benzophenone was recrystallized twice from absolute alcohol. The stearic acid and indium were used without further purification. All samples were weighed on an electrobalance[10] to the nearest 0.001 mg. Peak area measurements, when performed by planimetry, were repeated with a precision approaching 0.1%. The relative standard deviation for the area measurements ranged from 3.16% for indium fusion to 1.70% for stearic acid fusion.

Thermal Microscopy—Thermal microscopic examinations of the samples were performed on a Kofler micro hot stage[11]. A few sample particles were placed on a microscope slide and examined between crossed Nicols. A heating rate of 1° min^{-1} was used to determine transition temperatures. Known melting-point standards were utilized to check the thermometer calibration and the technique used. The magnification employed was 100×, and the numerical aperture was 0.25.

Scanning Electron Microscopy—Scanning electron micrographs[12] were obtained for each iopanoic acid form. Solid samples were coated with a thin gold film and maintained under a vacuum of 1×10^{-5} mm Hg. A 100-μm aperture was used to obtain magnifications of 1000–6000×.

IR Spectroscopy—Spectra of solid samples, prepared as potassium bromide[13] pellets in a miniature press[14], were recorded on a double-beam IR spectrophotometer[15]. A polystyrene film was used to check the spectrophotometer wavelength calibration. After the spectra were obtained, thermograms of the triturated and compressed samples were recorded to detect possible alterations in crystalline form due to the grinding operations and the pressures used.

Dissolution Studies—Powder dissolution profiles were obtained for each solid iopanoic acid form. A quantity of solute approximately equivalent to twice the saturation solubility was employed. No attempt was made to control particle size. The powder was added to 500 ml of preheated 0.02 *M* phosphate buffer solution, pH 6.50. The dissolution medium was stirred at 228 rpm with a stainless steel propeller, which was positioned 3 cm from the bottom of a USP dissolution flask. All experiments were performed at 37.0 ± 0.1°.

Fifteen-milliliter samples were withdrawn periodically through a me-

[6] Model 620005, Keuffel & Esser Co.
[7] MC & B Manufacturing Chemists, Norwood, Ohio.
[8] Supelco, Inc., Bellefonte, Pa.
[9] Fisher Scientific Co., Fair Lawn, N.J.
[10] Cahn G-2.
[11] Arthur H. Thomas Co.
[12] Stereoscan S4, Cambridge Instrument Co.
[13] Harshaw Chemical Co.
[14] Wilk's minipress.
[15] Perkin-Elmer 267.

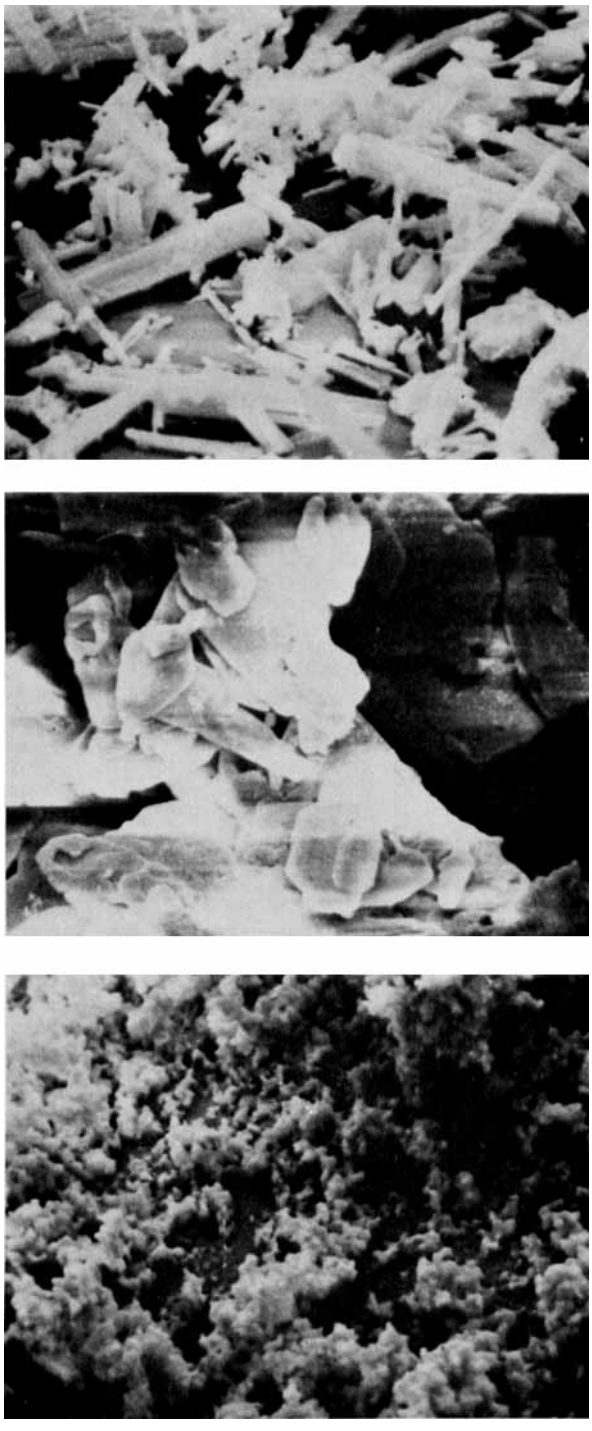

Figure 3 *Scanning electron micrographs of solid iopanoic acid forms. Key:* a, *Form I, magnification 1050×;* b, *Form II, magnification 1080×; and* c, *amorphous form, magnification 1200×.*

dium fritted glass disk, 3 cm in diameter. The volume withdrawn was immediately replaced with a equal volume of thermally equilibrated buffer. After appropriate dilution, samples were analyzed spectrophotometrically[16] at 230 nm, and a correction (13) was applied for the amount of solute removed during sampling.

Intrinsic dissolution rates also were determined. Approximately 500 mg of powder was placed in a 1.27-cm diameter flat-faced punch and die set and compressed under vacuum for 1 min with an applied load of 4545 kg[17]. The disk was removed from the die and mounted, with epoxy glue, in a glass tube, 2 cm in height and 1.27 cm in diameter, so as to expose only the upper surface of the pellet to the dissolution medium. Four extenders were attached to the bottom of the glass tube to stabilize the holder when it was placed in the dissolution medium. The intrinsic dissolution studies were carried out under sink conditions. All other experimental conditions and procedures were identical with those used in the powder dissolution studies.

[16] Cary model 14 or Gilford model 240.
[17] Carver laboratory press, model C.

RESULTS AND DISCUSSION

Three crystalline iopanoic acid forms and an amorphous form were obtained. With only one exception, all solvent systems used and all crystallization techniques attempted produced crystals identical with those of commercially available iopanoic acid (Form I). Crystals obtained by shock cooling a warm, saturated solution of iopanoic acid in benzene were identified as benzene solvate crystals. These crystals rapidly lost solvent when stored in air at room temperature.

Because the benzene solvate loses solvent to the atmosphere so quickly under ordinary temperature and pressure conditions, it is virtually impossible to obtain reproducible physical data on this form. Thermograms of the solvate are affected markedly by sample size and history, by heating rate, and by the tightness of the seal used on the sample pans. The typical thermogram of this form, however, is very similar to that of Form II, except for a broad, dual peak centered around 80°, the approximate benzene boiling point. When solvate crystals, after having been stored under a benzene atmosphere since preparation, are subjected to X-ray diffraction analysis, their X-ray pattern is essentially superimposable on that of Form II.

X-ray diffraction patterns of Forms I and II and of the amorphous form are shown in Fig. 1. The patterns indicate that the commercially available iopanoic acid (Form I) and Form II are both crystalline and that they are distinctly different. Peak positions and relative intensities for these forms are listed in Table I. Differences in peak positions and intensities can be attributed to alterations in the crystal lattice molecular arrangement. The X-ray pattern of the precipitated form, on the other hand, is characteristic of an amorphous solid. Identical patterns were obtained from "recently precipitated" iopanoic acid and from precipitated iopanoic acid that had been stored in a desiccator for more than 1 year. This observation is in contrast to that of Goldberger *et al.* (9), who reported that the dried precipitate is crystalline.

When longer radiation times and higher sensitivities were employed, peaks of low intensity were observed in some precipitated samples. Further analysis indicated that the peaks can be attributed to contamination of the largely amorphous material by Form I crystals. The degree of crystallinity in the precipitated samples is apparently a function of the iopanoic acid precipitation rate.

Thermograms of three solid forms are reproduced in Fig. 2. Sample weights of Form I and of the amorphous form varied from 12 to 17 mg, but smaller samples (7–9 mg) of Form II were used. Form I exhibits a single endothermic peak at 153.8°. The reported melting range for iopanoic acid is 152–158° (14). The Form II thermogram has a sharp endothermic peak at 132.6°, an exothermic peak at 141.2°, and a melting peak at 153.4°. The amorphous solid demonstrates a relatively small endothermic glass transition peak at 54.9°, a broad exothermic peak at 99.9°, and a melting peak at 153.2°. Over a two-year storage period, samples of both the amorphous form and of Form II underwent gradual transformations, which were reflected in minor changes in their thermograms.

Interpretation of the differential scanning calorimetry thermograms is facilitated by observations from thermal microscopy. Form I crystals are needle shaped; when examined between crossed Nicols, they exhibit a wide color spectrum. They begin to liquefy at 147°, and melting is complete at 155°. Kuhnert-Brandstatter (15), who employed a similar technique, reported a melting range of 148–155° for iopanoic acid.

Form II is plate-like and demonstrates birefringence when viewed between crossed polars. At 131°, its crystals begin to soften; in some samples, total liquefaction occurs at 135°. As the temperature is increased further, birefringent, needle-like crystals are formed, which eventually melt at 155°.

The amorphous powder is extremely electrostatic, and it is difficult to separate individual particles so that they can be examined microscopically. However, no distinct crystalline habit can be detected. As the temperature is increased to 50°, the centers of the particles become somewhat translucent, so that they acquire a donut-like appearance. At ~80°, the outer edges of the particles also become translucent. At >80°, there is virtually no change in appearance until melting occurs. No polarization of colors can be observed during the heating process.

Scanning electron micrographs of three solid forms are illustrated in

Table I—X-Ray Diffraction Patterns of Iopanoic Acid Forms I and II

Form I		Form II	
d, Å	I/I_1	d, Å	I/I_1
8.429	11.63	4.577	23.65
7.608	15.54	4.235	13.99
4.344	23.46	4.160	12.69
4.258	13.63	4.069	19.52
4.145	100.00	3.940	16.62
3.472	14.02	3.688	100.00
3.046	21.55	3.590	15.38
3.004	20.89	3.112	13.05
2.421	15.80	2.932	13.83
2.139	17.78	2.175	15.54

Fig. 3. The crystalline habits of Forms I and II can clearly be distinguished in these photomicrographs. The precipitated iopanoic acid, on the other hand, appears to be amorphous. Even at 6000-fold magnification, there is no evidence of crystallinity.

Differences in peak positions and in absorption intensities can be observed in the IR spectra of the various forms. Spectra of Form II and of the amorphous form are quite similar, with the largest difference being in the 910–940-cm^{-1} region, which is representative of carboxylic acid -OH out-of-plane bending (16). The two peaks at 1211 and 1295 cm^{-1} are both more intense in spectra of Forms I and II than in the spectrum of the amorphous form. These peaks have been attributed (16) to coupled -OH bending and C–O stretching of the carboxylic acid dimer and to C–N stretching, respectively. In addition, the NH symmetric stretching frequency at 3345 cm^{-1} can be used to distinguish Form I from the two other solid forms.

Results of the calorimetric studies are collected in Table II. The heats of transition were calculated from the equation:

$$\Delta H = \frac{K(A)}{m} \qquad \text{(Eq. 1)}$$

where ΔH is the enthalpy of transition, K is a calibration coefficient that is a function of temperature, A is the area of the transition peak, and m is the sample mass. The calibration coefficient is obtained by plotting $\Delta Hm/A$ *versus* the transition temperature for substances with known transition enthalpies (11). The precision reported here is comparable to that achieved by other authors employing similar techniques (17–19). Entropy changes associated with the transitions were obtained by dividing the transition enthalpy by the temperature in degrees Kelvin.

From the temperatures at which Form II and the amorphous form melt,

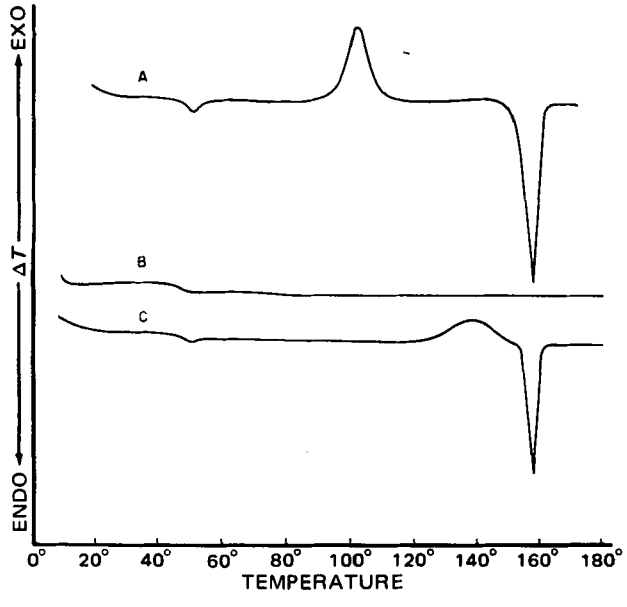

Figure 4—*Effect of thermal history and presence of seed crystals on differential scanning calorimeter thermograms for iopanoic acid. Key: A, typical thermogram of amorphous iopanoic acid; B, thermogram of the resolidified melt of the amorphous form; C, thermogram of the resolidified melt of the amorphous form following cooling in a dry ice–acetone mixture.*

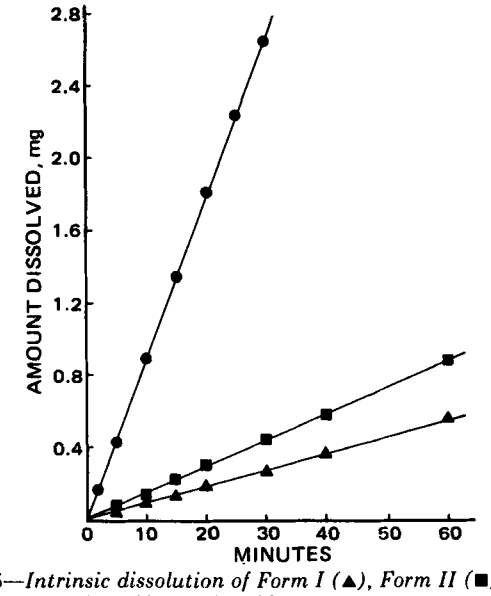

Figure 5—*Intrinsic dissolution of Form I (▲), Form II (■), and the amorphous form (●) of iopanoic acid.*

one can conclude that each is converted to Form I prior to final melting. However, a statistical test of the three ΔH_{fus} values at the 95% confidence level demonstrates a significant difference between the fusion enthalpy of Form II and of the two other forms. This discrepancy can be explained on the basis of incomplete Form I crystallization. The temperature at which the transition from Form II to Form I occurs is so close to the Form I melting point that, at the heating rates employed in this study, the transformation is incomplete when melting begins. This interpretation is corroborated by thermal microscopic observations.

Figure 4 illustrates the influence that seed crystals and thermal history can have on the transition temperature and on the exothermic peak observed in amorphous iopanoic acid thermograms. The top curve is a typical thermogram for the amorphous form heated from room temperature to beyond its melting point. Obviously, no seed crystals remain in this sample; when it is cooled, a glass forms. Curve B demonstrates the thermal behavior of the glass. A change in heat capacity is observed at approximately 48°; however, the typical exotherm and melt transition

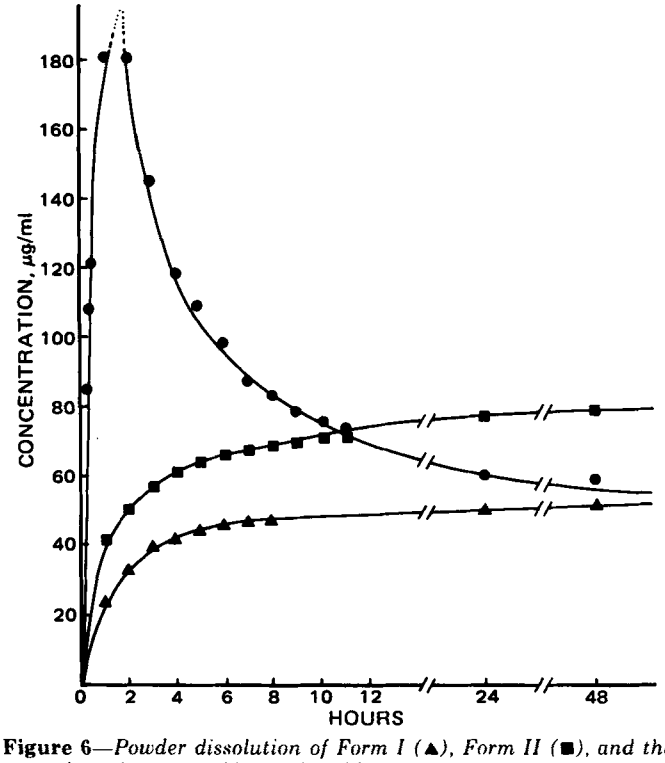

Figure 6—*Powder dissolution of Form I (▲), Form II (■), and the amorphous form (●) of iopanoic acid.*

Table II—Thermodynamic Data for Three Solid Iopanoic Acid Forms [a]

Form	Enthalpic Transition Type: Endothermic Temperature	Endothermic ΔH, kcal mole^{-1}	Endothermic ΔS, eu	Exothermic Temperature	Exothermic ΔH, kcal mole^{-1}	Exothermic ΔS, eu	Melt Temperature	Melt ΔH, kcal mole^{-1}	Melt ΔS, eu
Form I	—	—	—	—	—	—	153.8°	6.62	15.5
							±0.2°	±0.09	±0.2
Form II	132.6°	4.96	12.2	141.2°	−3.61	−8.71	153.4°	4.61	10.8
	±0.2°	±0.08	±0.2	±0.1°	±0.15	±0.15	±0.2°	±0.05	±0.1
Amorphous	54.9°	0.662	2.02	99.9°	−3.60	−9.65	153.2°	6.85	16.1
	±0.1°	±0.079	±0.02	±0.5°	±0.09	±0.23	±0.3°	±0.23	±0.5

[a] Values reported represent the mean and standard error of the mean of five to eight samples.

are not observed. When the glass is cooled in dry ice, it again exhibits an endothermic and exothermic transition, as well as the usual melting peak (curve C). In this case, however, the exotherm due to crystallization of Form I is broader and occurs at a higher temperature than in the original sample.

The results of the intrinsic dissolution rate studies are shown in Fig. 5. Assuming the dissolution rate is diffusion controlled, one can describe the process by:

$$\frac{1}{A}\frac{dW}{dt} = \frac{D}{h}(C_s - C) \qquad \text{(Eq. 2)}$$

where A is the surface area of the dissolving solid, W is the solute mass at time t, D is the diffusion coefficient, h is the diffusion layer thickness, C_s is the solubility of the substance, and C is its concentration in the bulk solution at time t. In the initial stages of the dissolution process, *i.e.*, when sink conditions prevail, $C_s \gg C$, and the equation reduces to:

$$\frac{1}{A}\frac{dW}{dt} = \frac{DC_s}{h} \qquad \text{(Eq. 3)}$$

All three solid iopanoic acid forms can be characterized by the same D and h values. In addition, the surface area of the dissolving disk is essentially constant, so Eq. 3 may be rewritten in a simpler form:

$$\frac{dW}{dt} = kC_s \qquad \text{(Eq. 4)}$$

where the constant k now includes the terms A, D, and h. Integration from time 0 to t yields:

$$W = kC_s t \qquad \text{(Eq. 5)}$$

Thus, a plot of amount dissolved as a function of time should be linear for the initial dissolution stages. Intrinsic dissolution rates (kC_s/A) can be calculated from the slopes of the three straight lines in Fig. 5. They are 0.00739 mg cm^{-2} min^{-1} for Form I, 0.0117 mg cm^{-2} min^{-1} for Form II, and 0.0703 mg cm^{-2} min^{-1} for the amorphous form. So the intrinsic dissolution rate for Form II is 1.5 times greater, whereas the dissolution rate for the amorphous form is an order of magnitude greater than that of the commercially available form.

Typical dissolution profiles for the three forms are shown in Fig. 6. The peak solubilities of the different forms follow the same rank order as their intrinsic dissolution rates, as predicted by Eq. 5. Form II is relatively stable in saturated aqueous solutions. The excess solid iopanoic acid remaining in the sample containers at the end of a dissolution run was predominantly Form II. With the amorphous form, on the other hand, there was appreciable conversion to Form I after only 2 hr, and conversion was essentially complete at the end of 12 hr of exposure to the dissolution medium.

Aguiar and Zelmer (20) employed the saturation concentrations obtained from powder dissolution profiles to predict whether a given metastable polymorph will demonstrate enhanced bioavailability. According to their hypothesis, differences in human absorption observed following administration of chloramphenicol polymorphs A and B can be explained on the basis of the relatively large (−774 cal mole^{-1}) free energy difference between the two forms. On the basis of the much smaller free energy difference (−231 cal mole^{-1}) between polymorphs I and II of mefenamic acid, the authors predicted that there would be no significant differences in the absorption of these two forms. Their prediction was borne out in subsequent *in vivo* tests.

By applying the Aguiar–Zelmer hypothesis to iopanoic acid, the free energy difference, ΔG, between two solid forms (*e.g.*, A and B) of the same compound can be obtained from:

$$\Delta G = RT \ln \frac{C_s \text{ Form B}}{C_s \text{ Form A}} \qquad \text{(Eq. 6)}$$

Since the saturation solubility, C_s, of each solid form, measured at the same temperature, is directly proportional to its intrinsic dissolution rate, the dissolution rate ratio can be substituted for the ratio of solubilities in Eq. 6. In the case of iopanoic acid, $\Delta G_{\text{II}\rightarrow\text{I},\,37°}$ is −284 cal mole^{-1}, and $\Delta G_{\text{amorphous}\rightarrow\text{I},\,37°}$ is −1390 cal mole^{-1}. Based on these calculations, it seems likely that the bioavailability of Form II should not be appreciably greater than that of Form I. In contrast, the bioavailability of the amorphous form should be considerably greater than that of the stable polymorph. While many other factors affect the optimal opacification of the bladder, it would be of interest to determine whether these thermodynamic data can be quantitatively correlated with bioavailabilities of the three forms.

REFERENCES

(1) H. J. Burhenne and W. G. Obata, *N. Engl. J. Med.*, **292**, 627 (1975).

(2) P. M. Loeb, R. N. Berk, J. O. James, L. Perkin, and J. Moore, *Radiology*, **126**, 395 (1978).

(3) R. G. Evens, C. Schroer, and P. R. Koehler, *ibid.*, **98**, 365 (1971).

(4) R. N. Berk, P. M. Loeb, L. E. Goldberger, and J. Sokoloff, *N. Engl. J. Med.*, **290**, 204 (1974).

(5) E. Gunnarson, *Acta Radiol.*, **52**, 289 (1959).

(6) K. Holmdahl and H. Lodin, *ibid.*, **51**, 247 (1959).

(7) P. Virtama, *ibid.*, **52**, 308 (1959).

(8) R. Peterhoff, *ibid.*, **46**, 719 (1956).

(9) L. E. Goldberger, R. N. Berk, J. H. Lang, and P. M. Loeb, *Invest. Radiol.*, **9**, 16 (1974).

(10) S. S. Yang and J. K. Guillory, *J. Pharm. Sci.*, **61**, 26 (1972).

(11) W. W. Wendlandt, "Thermal Methods of Analysis," 2nd ed., vol. 19 of "Chemical Analysis," P. J. Elving and I. M. Kolthoff, Eds., Wiley–Interscience, New York, N.Y., 1974, pp. 178–184.

(12) M. J. Richardson and N. G. Savill, *Thermochim. Acta*, **12**, 221 (1975).

(13) E. Nelson, *J. Am. Pharm. Assoc., Sci. Ed.*, **46**, 607 (1957).

(14) "The United States Pharmacopeia," 19th ed., Mack Publishing Co., Easton, Pa., 1975, p. 261.

(15) M. Kuhnert-Brandstätter, "Thermomicroscopy in the Analysis of Pharmaceuticals," Pergamon, New York, N.Y., 1971, p. 409.

(16) K. Nakanishi and P. H. Solomon, "Infrared Absorption Spectroscopy," 2nd ed., Holden-Day, San Francisco, Calif., 1977, p. 39.

(17) J. Y. C. Chu, *J. Phys. Chem.*, **79**, 119 (1975).

(18) M. J. Vold, H. Funakoshi, and R. D. Vold, *ibid.*, **80**, 1753 (1976).

(19) K. Konkoly-Thege, I. Ruff, S. O. Adeosun, and S. J. Sime, *Thermochim. Acta*, **24**, 89 (1978).

(20) A. J. Aguiar and J. E. Zelmer, *J. Pharm. Sci.*, **58**, 983 (1969).

ACKNOWLEDGMENTS

Presented in part at the Basic Pharmaceutics Section, APhA Academy of Pharmaceutical Sciences, Anaheim meeting, April 1979.

Iopanoic acid was generously provided by Dr. F. C. Nachod of the Sterling-Winthrop Research Institute. The authors thank Dr. Ching-Yuan Shih, Department of Botany, University of Iowa, who supervised the electron microscopy, and Dr. George R. McCormick, Department of Geology, University of Iowa, in whose laboratory the X-ray analysis was performed.

W. C. Stagner is a Charles J. Lynn Memorial Fellow, American Foundation for Pharmaceutical Education.